DOI: 10.1002/cssc.201200202

Controlling Surface Enrichment in Polymeric Hole Extraction Layers to Achieve High-Efficiency Organic Photovoltaic Cells

Dong-Hun Kim,[a] Kyung-Geun Lim,[a] Jong Hyeok Park,[b] and Tae-Woo Lee*[a]

Hole extraction in organic photovoltaic cells (OPVs) can be modulated by a surface-enriched layer formed on top of the conducting polymer-based hole extraction layer (HEL). This tunes the surface work function of the HEL to better align with the ionization potential of the polymeric photoactive layer. Results show noticeable improvement in device power conversion efficiencies (PCEs) in OPVs. We achieved a 6.1% PCE from the OPV by optimizing the surface-enriched layer.

Introduction

Academia and industry have shown great interest in organic photovoltaic cells (OPVs) based on printable polymeric semiconductors because of their potential as low-cost, light-weight, and flexible devices for sustainable solar energy conversion.[1,2] In recent years the power conversion efficiencies (PCEs) of polymer photovoltaic cells based on a blend of a polymer donor and a highly soluble fullerene derivative acceptor have drastically improved, mostly as a result of controlling the nanoscale morphology of the photoactive layer and by introducing new, tailor-made, low-band-gap polymers that have a broad range of light absorption.[2] Although many combinations of donor and acceptor materials have been tested as photoactive layer to increase the efficiency of OPVs, only a few polymeric materials have been tested as hole extraction layer (HEL).[3,4] Poly(3,4-ethylenedioxy thiophene) doped with poly(styrene sulfonate) (PEDOT:PSS) is still the most widely used because it can improve hole extraction from the photoactive layer due to its relatively high work function (WF $\approx$ 5.0–5.2 eV) compared to indium-doped tin oxide (ITO; WF $\approx$ 4.7–4.9 eV).[3] Hole extraction contact is an important issue, especially when the donor material in the photoactive layer has a highest occupied molecular orbital (HOMO) level that is lower than the WF of ITO, relative to the vacuum level.[5] Despite its importance for improving device efficiency the HEL has not been sufficiently studied yet. Many reports on the optimization of device performance lack a detailed investigation of the most-often used polymeric HEL (i.e., PEDOT:PSS). Therefore, the reported optimized processing conditions of the PEDOT:PSS layer in OPVs are different throughout the literature.[6] For example, the group of Heeger and Lee performed thermal annealing at 140 °C for 10 min, while the Yang group did so at 120 °C for 1 h.[6a,b] Kim et al. annealed the PEDOT:PSS layer of all OPV devices at a much higher temperature: 230 °C during 15 min.[6c,d] In addition to these differences in thermal annealing conditions, HELs with different PSS/PEDOT ratios have been used in OPVs, also.[6] Optimizations of device efficiency at different HEL annealing temperatures and PSS/PEDOT ratios are done without a clear understanding of why specific experimental conditions result in the best device performance.

In this study, the HEL surface has been controlled in a systematic manner, so as to clarify the effect of the surface layer on device performance. First, we varied the temperature at which the PEDOT:PSS HEL films are heat-treated. Second, we varied the PSS/PEDOT ratio of the HEL solution to control the PSS-enriched surface layer of spin-cast HEL films. We found a lucid connection between the surface WF tuned by the PSS-enriched surface layer and device performance parameters, such as open-circuit voltage (V_{oc}), short-circuit current (J_{sc}), fill factor (FF), and PCE. The PSS-enriched surface layer in PEDOT:PSS film actually controls the surface WF and thus hole extraction from the photoactive layer (Figure 1). We investigated the effect of the PSS-enriched surface layer of the PEDOT:PSS film on the surface WF and hole extraction capability by using ultraviolet photoelectron spectroscopy (UPS) and X-ray photoelectron spectroscopy (XPS).

Results and Discussion

In order to study the contribution of the PSS surface layer to the tuning of the HEL WF, the HEL heat treatment was applied to systems with two different photoactive materials: poly(3-hexylthiophene):[6,6]-phenyl-C_{61}-butyric acid methyl ester (P3HT:PCBM) and poly(*N*-9′-hepta-decanyl-2,7-carbazole-alt-5,5-(4′,7′-di-2-thienyl-2′,1′,3′-benzothiadiazole):[6,6]-phenyl-C_{70}-bu-

[a] *D.-H. Kim,[+] K.-G. Lim,[+] Prof. T.-W. Lee*
Department of Materials Science and Engineering,
Pohang University of Science and Technology (POSTECH)
San 31, Hyoja-dong, Nam-gu, Pohang, Gyeongbuk 790-784 (Korea)
Fax: (+82) 54-279-2399
E-mail: twlee@postech.ac.kr

[b] *Prof. J. H. Park*
School of Chemical Engineering and
SKKU Advanced Institute of Nanotechnology (SAINT)
Sungkyunkwan University
Suwon 440-746 (Korea)

[+] *These authors contributed equally to this work.*

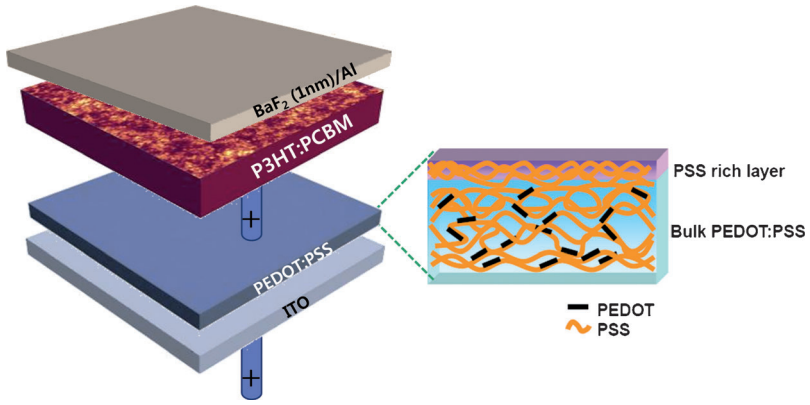

Figure 1. Schematic device structure of organic bulk heterojunction photovoltaic cells and schematic morphology of vertically phase-segregated PEDOT:PSS with a PSS-rich layer.

tyric acid methyl ester (PCDTBT:$PC_{70}BM$). A layer of PEDOT:PSS of ca. 25 nm thickness was spin-coated on top of an ITO/glass substrate. After the ITO/PEDOT:PSS was thermally annealed at various temperatures in order to control the surface composition of the PSS-enriched surface, the P3HT:PCBM or PCDTBT:$PC_{70}BM$ photoactive layer was spin-coated onto the PEDOT:PSS layer. Figure 2a shows current density–voltage (*J–V*) characteristics of the devices. With increasing PEDOT:PSS annealing temperature, from 110 to 200 °C, the V_{oc} did not change while J_{sc} and the FF increased, which improved the PCE. The PCE of the device annealed at 110 °C was the lowest (2.4 %) among all samples. The PCE of the OPV devices was highest (3.5 %) at an annealing temperature of 200 °C.

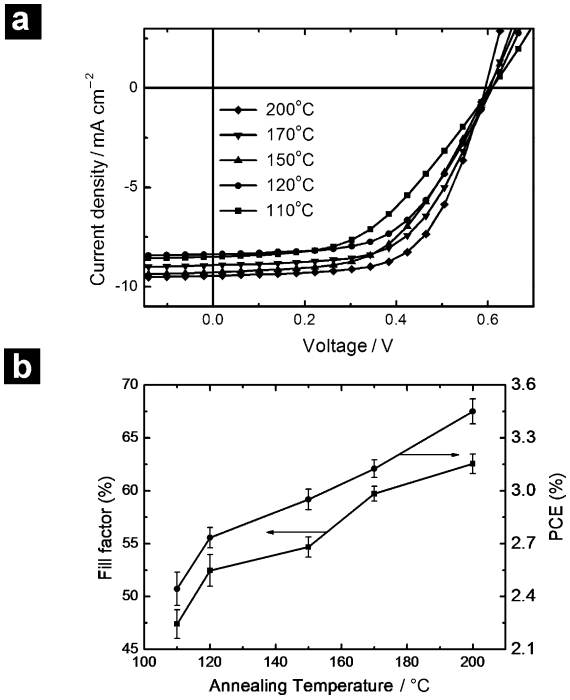

Figure 2. a) Current density versus voltage characteristics of P3HT:PCBM organic photovoltaic cells illuminated under 1.5AM 100 mW cm^{-2} with varying the annealing temperatures of PEDOT:PSS layer. b) Device power conversion efficiencies and fill factors depending on annealing temperatures of PEDOT:PSS.

We tried to understand the PCE enhancement by probing the surface composition and WF of the annealed PEDOT:PSS layers. X-ray photoelectron spectroscopy (XPS) was used because it can provide valuable information on the surface composition of the PEDOT:PSS films annealed at various temperatures (Figure 3). It is well-established that a PSS-rich layer results after spin-casting of PEDOT:PSS because of phase segregation, with an excess of PSS in the surface region.[7–10] Figure 3 shows S 2p core level spectra of PEDOT:PSS films annealed at 110, 150, and 200 °C. The S 2p peak usually consists of a two-spin-split doublet, S $2p_{1/2}$ and S $2p_{3/2}$, with an energy splitting of 1.20 eV. The higher-binding-energy peak at ca. 169 eV is assigned to the sulfur atoms in PSS, and the lower one at ca. 164 eV is assigned to the sulfur atoms in PEDOT, based on well-established

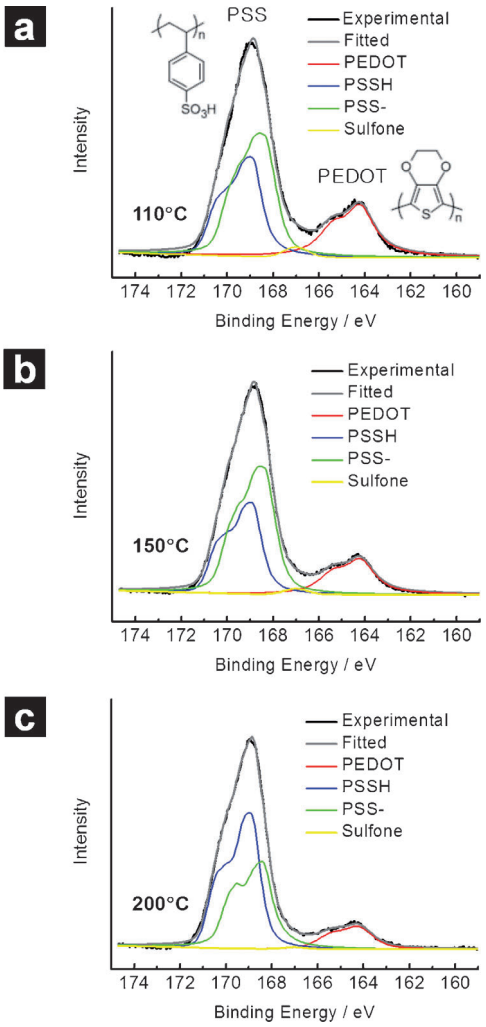

Figure 3. S 2p core level spectrum of PEDOT:PSS varying annealing temperatures a) 110 °C, b) 150 °C, and c) 200 °C.

XPS studies on PEDOT:PSS films.[7–10] The peaks at 168.4 and 168.9 eV correspond to the PSS^- salt and PSSH, respectively.[8] In addition, a very small peak at about ca. 167 eV was added for satisfactory fitting, which can be assigned to an intermediate state, sulfone ($-SO_2-$).[9] The ratios of PSS/PEDOT were calculated by using the area ratios under the two different peaks and are shown in Table 1. Surprisingly, the PSS/PEDOT ratio at the HEL surface consistently increased with increasing HEL annealing temperature. At 110 °C, the PSS/PEDOT ratio was only 3.675, but at 200 °C, the ratio was 8.397, more than double. This indicates that thermal annealing can control the concentration of the surface-enriched layer.

Table 1. The effect of thermal annealing temperature on the work function of PEDOT:PSS films, the PSS/PEDOT ratio at the film surface, and the power conversion efficiencies of P3HT:PCBM OPVs using the PEDOT:PSS films.

Annealing temperature [°C]	Work function [eV]	PSS/PEDOT ratio at surface	PCE [%]
110	4.91	3.675	2.44 ± 0.09
120	4.95	4.065	2.73 ± 0.06
150	5.01	5.065	2.95 ± 0.06
170	5.04	8.169	3.13 ± 0.05
200	5.05	8.397	3.45 ± 0.07

As the annealing temperature increased, the series resistance (R_s) decreased from 28.8 $\Omega\,cm^2$ at 110 °C to 14.8 $\Omega\,cm^2$ at 200 °C. The FF and J_{sc} also increased in spite of increased PSS surface concentration. This can be explained in terms of increasing PEDOT:PSS conductivity[6e] and p-doping of P3HT by the PSS surface layer.[6f] Upon annealing, the insulating PSS chains that are not bound to PEDOT will be phase-segregated from the conducting PEDOT:PSS grains and migrate toward the film surface. This makes the annealed PEDOT:PSS more conductive,[6e] which can decrease R_s. Huang et al. reported p-doping of P3HT by PSS at the PEDOT:PSS/P3HT interface upon heating.[6f] Therefore, even if thermal annealing generates an insulating PSS layer at the film surface, some portion of PSS enriched at the surface of the annealed PEDOT:PSS film induces doping of P3HT during heating, which facilitates hole extraction via the PSS surface layer.

In an earlier work, we found that the luminous current efficiency in polymer light-emitting diodes is strongly affected by the surface WF of the films spin-cast from various PEDOT:PSS compositions.[9] The surface WF of PEDOT:PSS films was tuned by controlling the molecular weight of PSS and the relative bulk concentration of PSS to PEDOT in PEDOT:PSS.[9] The surface WF consistently increased as the ratio of PSS to PEDOT in the composition increased. In the present work, we demonstrate that the surface WF of single PEDOT:PSS composition can also be tuned by adjusting the thermal annealing temperature to control the degree of surface segregation of PSS. UPS measurements of the surface WF of PEDOT:PSS film show a systematic increase of the WF as the annealing temperature increased (Figure 4). The surface WF of PEDOT:PSS steadily increased as the PSS/PEDOT ratio increased and tended to saturate when the ratio was more than 8 (Figure 4). Overall, we found that the surface segregation of PSS in PEDOT:PSS layer could be controlled by various heat treatments. Not only heating temperatures, but also heating time might affect the surface segregation of PSS,[11] although experiments with varying heating times were not conducted.

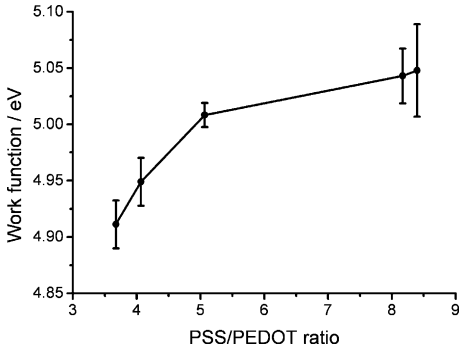

Figure 4. Effect of PSS/PEDOT ratio at the film surface on the film WF.

In addition, PEDOT:PSS layers heated at various temperatures from 110 to 220 °C were applied to PCDTBT:PC_{70}BM OPVs. Figure 5a shows the *J–V* characteristics of these devices. With increasing PEDOT:PSS annealing temperature, from 110 to 220 °C, the V_{oc} and J_{sc} slightly increased (Figure 5b). Because the PSS enrichment at the PEDOT:PSS surface increased with thermal annealing temperature, the surface WF also increased with thermal annealing temperature (Figure 4). As the PEDOT:PSS WF increased at a given thermal annealing temperature, the energy level difference between the WF of PE-

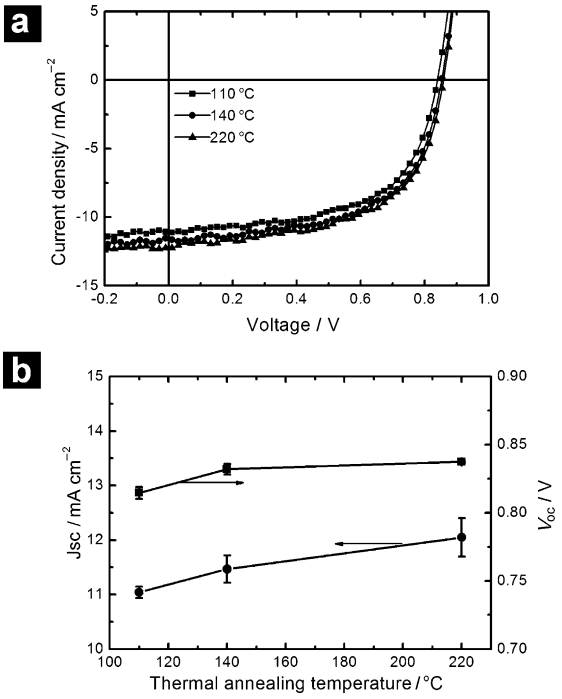

Figure 5. a) Current density versus voltage, and b) J_{sc} and V_{oc} characteristics of PCDTBT:PC_{70}BM organic photovoltaic cells illuminated under 100 mW cm^{-2} vs. annealing temperatures of PEDOT:PSS layer.

DOT:PSS and the ionization potential of PCDTBT decreased and the built-in potential (V_{bi}) between the PEDOT:PSS and the cathode accordingly increased. Therefore, V_{oc} increased when the WF-enhanced PEDOT:PSS layer was used in the PCDTBT:$PC_{70}BM$ device. Especially, a slight increment of V_{oc} at high thermal annealing temperature can be obtained in the PCDTBT:$PC_{70}BM$ device, but not in the P3HT:PCBM device. The reason for the almost fixed V_{oc} in the P3HT:PCBM device (Figure 2) is that the WF of PEDOT:PSS (4.9–5.0 eV) is already pinned to the ionization potential of P3HT (ca. 5.0 eV), in spite of the WF increment of the heated PEDOT:PSS.[12] Earlier work has shown that even a much higher WF of the HEL (ca. 5.8 eV) becomes pinned to the ionization potential of the donor polymer (P3HT) in P3HT:PCBM devices, thus fixing the V_{oc} while J_{sc} increased very slightly.[12a] In contrast, PCDTBT has a much higher ionization potential (ca. 5.4 eV) than P3HT, and the increase in V_{oc} is more apparent in the PCDTBT:$PC_{70}BM$ device than in the P3HT:PCBM device. In addition, hole extraction from the photoactive layer to ITO is much easier because of a better match between the WF of PEDOT:PSS annealed at a higher temperature and the HOMO level of the PCDTBT; this results in an increase of the built-in electric field in addition to a higher conductivity of PEDOT:PSS film annealed at higher temperature and further p-doping of PCDTBT at the interface by more surface-enriched PSS. This improved hole extraction interface can improve the J_{sc} in addition to V_{oc} so that the PCE increases, from 5.5 to 6.1%.

The PSS concentration at the surface is controllable in a wider range by increasing the PSS/PEDOT ratios of the HEL compositions[9] than by heat treatment of the pristine HEL composition. As another way to control the HEL surface, the PSS/PEDOT ratio in the solution was controlled from conventional (1:2.5) to higher ratios. Figure 6a shows *J–V* characteristics of PCDTBT:$PC_{70}BM$ devices using several different PEDOT:PSS compositions. Six different compositions were tested, with PEDOT:PSS weight ratios of 1:2.5, 1:3.5, 1:5, 1:8, 1:12, and 1:16. In a previous study, it has been reported that as the PSS ratio in the PEDOT:PSS solution was increased from 1:2.5 to 1:20, the WF at the PEDOT:PSS surface was increased.[13] The surface WF is correlated to the PSS concentration at the film surface.[9] Therefore, the increase in V_{oc} of the device with increased PSS ratio in the PEDOT:PSS (Figure 6b) can be attributed to an increase in the WF of the PEDOT:PSS film surface with an increase in this ratio.

As we increased the PSS/PEDOT ratio of the compositions, we observed a further increase of the V_{oc} up to 0.906 V at the 1:12 ratio (Figure 6b). The saturation of V_{oc} indicates that the WFs of the HELs become closer to the ionization potential of the PCDTBT as the PSS concentration increases. In contrast, J_{sc} was almost independent of the PEDOT:PSS ratio; this indicates that even a high concentration of PSS at the film surface (or increased surface layer thickness) and inside the film (or lowered film conductivity) did not significantly prevent hole extraction, despite the electrically insulating nature of PSS. This can be understood on the basis of a better alignment of HEL WFs with the ionization potential of PCDTBT to increase the built-in field and on the doping effect of PSS at the interface of HEL/PCDTBT upon heating,[6f] which can compensate for the negative effect of increased concentration of insulating PSS on hole extraction in the HEL. Based on previous literature,[7,9] the PSS-rich layer on the film surface was thinner than 3 nm. However, when we further increased the thickness of the PSS surface layer enriched at the film surface, the effect of increased hole extraction due to the increased built-in field across the active layer caused by increased film WF and p-doping by PSS competed with hole blocking by the thicker insulating PSS surface layer. The PCE was maximized at the PEDOT:PSS ratio of 1:3.5; this device had saturated V_{oc} and the highest J_{sc}. As PSS concentration in the composition was increased above this ratio, we found a very slight gradual decrease of the J_{sc} and PCE. However, it is noted that all the OPV devices using reformulated PEDOT:PSS with higher PSS content showed higher PCEs than the control device. This indicates the importance of the surface composition to increase the surface WF and thus V_{oc} in OPVs.

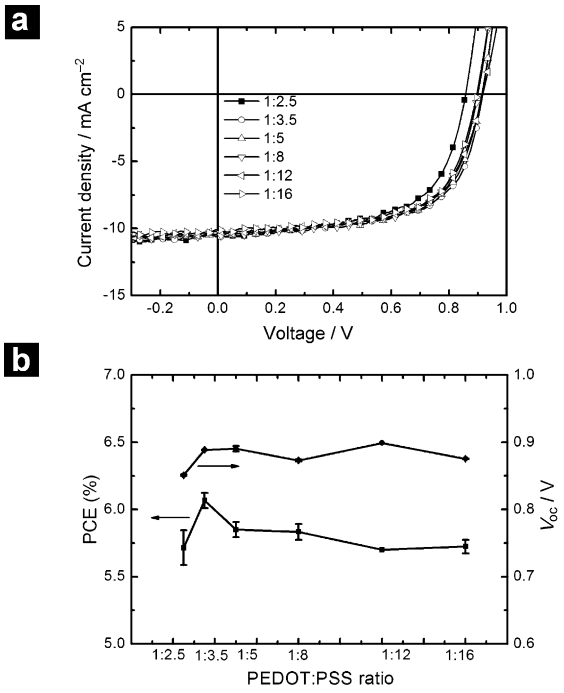

Figure 6. Characteristics of PCDTBT:$PC_{70}BM$ organic photovoltaic cells with differing PSS/PEDOT ratios. a) Current density versus voltage, and b) V_{oc}, J_{sc}, FF, and PCE characteristics under 100 mW cm^{-2} illumination vs. PSS ratio of PEDOT:PSS solution.

Conclusions

We modulated the vertically segregated PSS-enriched layer at the surface of PEDOT:PSS films by adjusting the thermal annealing temperature and PSS ratio of the PEDOT:PSS composition. We showed how the surface layer affects the overall OPV device performance parameters. As the annealing temperature of the PEDOT:PSS layer increased, the PSS/PEDOT ratio at the surface increased, which also resulted in an increased surface work function and a better alignment of the hole extraction layer work function with the ionization potential of PCDTBT,

and consequently increased V_{oc}, J_{sc}, and power conversion efficiency values in organic photovoltaics that use a PCDTBT:$PC_{70}BM$ photoactive layer. Furthermore, as the PSS ratio in the PEDOT:PSS compositions increased, the V_{oc} increased due to the increase in surface work function and then saturated. Finally, we achieved noticeably improved power conversion efficiencies in organic photovoltaics (6.1%). This work demonstrates that a PSS-enriched surface of the hole extraction layer is important to improve the hole extraction, the V_{oc}, and thus the overall power conversion efficiency of the organic photovoltaic device. These findings are widely applicable and can be used to improve charge injection in other organic electronic devices such as organic light-emitting diodes or organic transistors.

Experimental Section

The photovoltaic cells were fabricated on precleaned ITO/glass substrates. First, PEDOT:PSS (Baytron PH) was spin-coated to an average thickness of 25 nm. Then, the samples were annealed at various temperatures to clarify the effect of HEL annealing temperature on the device performance parameters. The annealing temperatures varied from 110 to 220 °C, and the annealing time was 10 min. In addition, the PSS ratio in PEDOT:PSS solution was modulated from 1:2.5 to 1:16 by adding PSS ($M_w \approx 75\,000$, Sigma Aldrich). PEDOT:PSS with various PSS ratios was spin-coated and thermally annealed at 200 °C for 10 min. A blend of P3HT (RR 90–94%, M_w 55 000–60 000, Rieke 4002-EE) and PCBM (purity 99.5%, M_w 910.9, Nano-c) (20 mg each) in 1.5 mL dichlorobenzene (DCB) was prepared for the photoactive layer and heated at 60 °C for 12 h before spin-coating. Another blend of PCDTBT (1-material, 7 mg) and $PC_{70}BM$ (Nano-c, 28 mg) in 1 mL DCB was also prepared for the photoactive layer. After that, all the substrates were transferred to a N_2 glove box in which the photoactive layers were spin-coated on top of the HELs. P3HT:PCBM layers were spin-coated at 900 rpm for 5 s to make films of 210 nm thickness. PCDTBT:$PC_{70}BM$ layers were spin-coated at 1600 rpm for 60 s to make films of 80 nm thickness. Then, the P3HT:PCBM layer and the PCDTBT:$PC_{70}BM$ layer were thermally annealed at 150 °C and 70 °C, respectively, for 10 min in an N_2 glove box. After transferring all of the samples to a thermal evaporator with high vacuum (ca. 1×10^{-7} torr), an Al electrode (100 nm thick) was deposited after interlayer deposition of 1 nm-thick BaF_2 for P3HT:PCBM and 3 nm-thick Ca for PCDTBT:$PC_{70}BM$. A UV-curable epoxy resin was used to encapsulate the cells with glass lids. All device parameters including power conversion efficiency were measured under illumination at AM 100 mW cm^{-2} generated using a solar simulator (Newport 69907). The vertical compositions of PSS in PEDOT:PSS film were obtained by using synchrotron X-ray photoelectron spectroscopy (XPS) at Pohang Accelerator Laboratory, and the work functions of PEDOT:PSS layers were measured by using a home-built ultraviolet photoemission spectroscope at POSTECH.

Acknowledgements

This research was supported by the Basic Research Program through the National Research Foundation of Korea (NRF), funded by the Ministry of Education, Science and Technology (No. 2010-0026281). This work was also supported by a grant (No. 2011-0031639) from the Center for Advanced Soft Electronics under the Global Frontier Research Program of the Ministry of Education, Science, and Technology, Korea.

Keywords: conducting polymers · hole extraction · interfaces · solar cells · surfaces

[1] a) M. Pagliaro, R. Ciriminna, G. Palmisano, *ChemSusChem* **2008**, *1*, 880–891; b) B. C. Thompson, J. M. J. Frechet, *Angew. Chem.* **2008**, *120*, 62–82; *Angew. Chem. Int. Ed.* **2008**, *47*, 58–77; c) T.-W. Lee, K.-G. Lim, D.-H. Kim, *Electron. Mater. Lett.* **2010**, *6*, 41–50; d) R. Steim, F. R. Koglera, C. J. Brabec, *J. Mater. Chem.* **2010**, *20*, 2499–2512; e) J. H. Park, T.-W. Lee, B.-D. Chin, D. H. Wang, O. O. Park, *Macromol. Rapid Commun.* **2010**, *31*, 2095–2108; f) M. H. Yun, G.-H. Kim, C. Yang, J. Y. Kim, *J. Mater. Chem.* **2010**, *20*, 7710–7714.

[2] a) W. Cai, X. Gong, Y. Cao, *Sol. Energy Mater. Sol. Cells* **2010**, *94*, 114–127; b) M. Helgesen, R. Søndergaard, F. C. Krebs, *J. Mater. Chem.* **2010**, *20*, 36–60; c) C. J. Brabec, S. Gowrisanker, J. J. M. Halls, D. Laird, S. Jia, S. P. Williams, *Adv. Mater.* **2010**, *22*, 3839–3856; d) G. Dennler, M. C. Scharber, C. J. Brabec, *Adv. Mater.* **2009**, *21*, 1323–1338; e) J. Jo, S.-I. Na, S.-S. Kim, T.-W. Lee, Y. Chung, S.-J. Kang, D. Vak, D.-Y. Kim, *Adv. Funct. Mater.* **2009**, *19*, 2398–2406; f) H. J. Kim, J. W. Kim, J.–J. Kim, *Electron. Mater. Lett.* **2011**, *7*, 93–104.

[3] a) P. Ravirajan, D. D. C. Bradley, J. Nelson, S. A. Haque, J. R. Durrant, H. J. P. Smit, J. M. Kroon, *Appl. Phys. Lett.* **2005**, *86*, 143101; b) C. J. Ko, Y.-K. Lin, F.-C. Chena, C.-W. Chu, *Appl. Phys. Lett.* **2007**, *90*, 063509; c) T. M. Brown, J. S. Kim, R. H. Friend, F. Cacialli, R. Daik, W. J. Feast, *Appl. Phys. Lett.* **1999**, *75*, 1679–1681.

[4] a) C.-Y. Li, T.-C. Wen, T.-F. Guo, *J. Mater. Chem.* **2008**, *18*, 4478–4482; b) B. Kang, L. W. Tan, S. R. P. Silva, *Appl. Phys. Lett.* **2008**, *93*, 133302; c) A. W. Hains, T. J. Marks, *Appl. Phys. Lett.* **2008**, *92*, 023504.

[5] H.-Y. Chen, J. Hou, S. Zhang, Y. Liang, G. Yang, Y. Yang, L. Yu, Y. Wu, G. Li, *Nat. Photonics* **2009**, *3*, 649–653.

[6] a) S. H. Park, A. Roy, S. Beaupre, S. Cho, N. Coates, J. S. Moon, D. Moses, M. Leclerc, K. Lee, A. J. Heeger, *Nat. Photonics* **2009**, *3*, 297–303; b) G. Li, V. Shrotriya, J. Huang, Y. Yao, T. Moriarty, K. Emery, Y. Yang, *Nat. Mater.* **2005**, *4*, 864–868; c) Y. Kim, S. A. Choulis, J. Nelson, D. D. C. Bradley, S. Cook, J. R. Durrant, *Appl. Phys. Lett.* **2005**, *86*, 063502; d) Y. Kim, A. M. Ballantyne, J. Nelson, D. D. C. Bradley, *Org. Electron.* **2009**, *10*, 205–209; e) B. Friedel, P. E. Keivanidis, T. J. K. Brenner, A. Abrusci, C. R. McNeill, R. H. Friend, N. C. Greenham, *Macromolecules* **2009**, *42*, 6741; f) D. M. Huang, S. A. Mauger, S. Friedrich, S. J. George, D. Dumitriu-LaGrange, S. Yoon, A. J. Moulé, *Adv. Funct. Mater.* **2011**, *21*, 1657–1665.

[7] J. Hwang, F. Amy, A. Kahn, *Org. Electron.* **2006**, *7*, 387–396.

[8] G. Greczynski, Th. Kugler, W. R. Salaneck, *Thin Solid Films* **1999**, *354*, 129–135.

[9] T.-W. Lee, Y. Chung, *Adv. Funct. Mater.* **2008**, *18*, 2246–2252.

[10] a) T.-W. Lee, Y. Chung, O. Kwon, J.-J. Park, *Adv. Funct. Mater.* **2007**, *17*, 390–396; b) T.-H. Han, Y. Lee, M.-R. Choi, S.-H. Woo, S.-H. Bae, B. H. Hong, J.-H. Ahn, T.-W. Lee, *Nat. Photonics* **2012**, *6*, 105–110; c) M.-R. Choi, S.-H. Woo, T.-H. Han, K.-G. Lim, S.-Y. Min, W. M. Yun, O. K. Kwon, C. E. Park, K.-D. Kim, H.-K. Shin, M.-S. Kim, T. Noh, J. H. Park, K.-H. Shin, J. Jang, T.-W. Lee, *ChemSusChem* **2011**, *4*, 363–368; d) T.-W. Lee, O. Kwon, M.-G. Kim, S. H. Park, J. Chung, S. Y. Kim, Y. Chung, J.-Y. Park, E. Han, D. H. Huh, J.-J. Park, L. Pu, *Appl. Phys. Lett.* **2005**, *87*, 231106.

[11] P. C. Jukes, S. J. Martin, A. M. Higgins, M. Geoghegan, R. A. L. Jones, S. Langridge, A. Wehrum, S. Kirchmeyer, *Adv. Mater.* **2004**, *16*, 807.

[12] a) M.-R. Choi, T.-H. Han, K.-G. Lim, S.-H. Woo, D. H. Huh, T.-W. Lee, *Angew. Chem.* **2011**, *123*, 6398–6401; *Angew. Chem. Int. Ed.* **2011**, *50*, 6274–6277; b) R. M. Cook, L.-J. Pegg, S. L. Kinnear, O. S. Hutter, R. J. H. Morris, R. A. Hatton, *Adv. Energy Mater.* **2011**, *1*, 440.

[13] N. Koch, A. Elschener, J. P. Rabe, R. L. Johnson, *Adv. Mater.* **2005**, *17*, 330–335.

Received: March 22, 2012
Revised: May 2, 2012
Published online on September 3, 2012

